Comparison of two methods to provide highly resolved atmospheric turbulence data for simulations of wing and nacelle circulations

Carolin Helmke [*1], Torsten Auerswald [†2],
Siegfried Raasch [‡1], Jens Bange [§2]

[1] *Institute of Meteorology and Climatology, Leibniz Universität Hannover, Germany*

[2] *Institute for Geoscience, Eberhard Karls Universität Tübingen, Germany*

Abstract

Small scale atmospheric turbulence may play an important role for stall effects. Atmospheric turbulence in numerical models for calculating the flow around airfoils, wings and nacelles is typically generated from very simple stochastic models. These models generally do not account for the wide variety of atmospheric conditions.

A more advanced method is to generate synthetic three-dimensional turbulent wind fields from one-dimensional real flight measurements (time series data) in the atmosphere. Measured statistical properties like the energy spectrum, correlation matrix and velocity variances are used to generate these synthetic fields. Another but very expensive method is to explicitly simulate the three-dimensional turbulent wind fields using large-eddy simulation (LES). This paper compares both methods. Synthetic three-dimensional fields are generated from time series data which are taken from virtual flights within the LES. This allows a precise evaluation of the quality of the synthetically generated fields, because they should show the same features as the simulated fields from LES.

Statistical properties of the compared fields are in good agreement whereas typical coherent structures of boundary layers, i.e. thermals, convergence lines or low level jets, cannot be reproduced. Also dependencies of properties on height, e.g. for variances or turbulent fluxes, and the non-Gaussian distribution of the vertical velocity are missing in synthetic fields.

Both wind fields will later be used to initialize a numerical model for investigations of stall effects in order to analyze the general effects of air turbulence on wings and to find out differences caused by the two methods.

[*]Dipl.-Met.
[†]Dipl.-Met.
[‡]Prof. Dr.
[§]Prof. Dr.

Nomenclature

d_{sf}	grid spacing of the synthetic field [m]
d_{vf}	grid spacing of the virtual measurement [m]
k_{max}	maximum resolved wavenumber [1/m]
θ	potential temperature [K]
u	streamwise velocity component [m/s]
v	spanwise velocity component [m/s]
w	vertical velocity component [m/s]
x	streamwise Cartesian coordinate
y	spanwise Cartesian coordinate
z	vertical Cartesian coordinate
z_i	height of the atmospheric boundary layer [m]

1 Introduction

Investigations of stall effects are an important task for optimizing air traffic. Especially during approach knowledge of the stall can extend the limits of flyable ranges resulting in a reduction of noise immission or an increase of the flight frequency under safety conditions.
High risks and costs of flight experiments generally do not allow the testing of limits and can even prohibit developments of innovative configurations. Therefore numerical simulations of the flow around airfoils, wings and nacelles play an important role for investigations of stall effects.
During approach aircrafts pass the atmospheric boundary layer (ABL), the first 1-2 km of the troposphere in height with predominant turbulent flows. The ABL contacts the surface and responds to changing conditions, e.g. radiation or roughness, within a few hours. Resultant turbulent flows may strongly influence stall effects of aircrafts. Usually, numerical models for flows around wings provide atmospheric turbulence merely with the help of statistical models. Such generated data do not account for the wide range of different atmospheric flows. Turbulence in the atmosphere is often non-Gaussian distributed and coherent structures occur. The flow also strongly depends on height.
Two new methods are developed and compared to provide three-dimensional realistic turbulent wind fields. The first method uses explicitly simulated three-dimensional turbulent wind fields from LES. The second method generates synthetic three-dimensional wind fields from statistical properties derived from one-dimensional horizontal flight measurements (time series data). In this study, we are replacing the measurements by virtual measurements, carried out within the simulated wind field of the LES. This allows us to directly compare the simulated and the synthetically generated wind fields and hence to verify the second (synthetic) method, as well as to point out the differences between both methods, respectively.

1.1 Highly resolved LES wind fields

The parallelized LES model PALM is used for the first method. It simulates highly resolved atmospheric boundary layer flows under realistic conditions. The resulting flows reproduce all structures typical for each meteorological scenario e.g. non-Gaussian distributions of turbulence features, coherent structures like thermals or convergence lines and low level jets.

Flow fields of three different meteorological scenarios are simulated. A convective boundary layer with and without mean background wind as well as a stably stratified boundary layer. We had to limit ourselves to a few exemplary scenarios, since highly resolved LES of the atmosphere are computationally very expensive.

1.2 Synthetic wind fields from flight measurements

The second method to provide atmospheric turbulence data for numerical simulations of wing circulations is more advanced than earlier stochastic models. The synthetic method generates three-dimensional turbulent wind fields from one-dimensional measurements. Usually, the measurement data are taken using the airborne measurement system Helipod [1] [2]. With the Helipod measurement flights are performed during different meteorological scenarios in the real atmosphere. Statistical properties, i.e. energy spectrum, variances and the correlation matrix of the velocity components, are extracted from the measured time series data in order to generate the three-dimensional synthetic wind fields, which show turbulence statistics very similar to the measurements. Auerswald [3] describes the method in detail.
In our study, the measured data are replaced by virtual data from virtual flight measurements within the highly resolved LES wind fields. The virtual measurement method has been described in detail by Schröter et al. [4]. The synthetically generated fields obtained from these virtual measurements are compared with the explicitly simulated LES fields from the first method. This approach allows us to evaluate the quality of the second synthetic method precisely, because ideally, the synthetic fields should show the same features as the explicitly simulated LES fields.

The next section gives detailed descriptions of the LES model PALM, the selected simulations and the realization of the virtual flight measurements. Results of the comparison are presented in section 3 while a conclusion completes this paper (section 4).

2 PALM - parallelized LES model

This study uses the **pa**rallelized **L**ES **m**odel PALM developed by Raasch and Schröter [5]. It is a model for the atmosphere or oceanic boundary layer. PALM is written in Fortran 95 with single processor optimization for different processor architectures and uses MPI and/or OpenMP for parallelization.
PALM calculates the non-hydrostatic, incompressible Boussinesq equations, the 1st law of thermodynamics and equations for subgrid-scale (SGS) turbulent kinetic energy (TKE) and scalar conservation. Equations are discretized using finite differences. They are filtered implicitly following the volume-balance approach [6]. Turbulence closure uses the $1\frac{1}{2}$th order Deardoff [7] scheme.
Variables are staggered according to the marker-and-cell method/Arakawa C grid [8] [9]. Available advection schemes include the default second-order Piacsek-Williams [10] and a monotone scalar advection scheme [11] [12]. Available time integration schemes are 2nd and default 3rd-order Runge-Kutta, Euler and the leap-frog scheme. Incompressibility is ensured by the fractional step method, and the resulting Poisson equation for the perturbation pressure is solved by the default FFT or a multigrid pressure solver. For this study, the Runge-Kutta, Piacsek-Williams, and FFT-scheme is used respectively.
Concerning boundary conditions, cyclic conditions are used along the horizontal directions.

For the velocity components, all simulations use Monin-Obukhov similarity at the bottom and Dirichlet conditions at the top boundary. The convective cases use a homogeneous heating (kinematic sensible heatflux = 0.24 K m/s) and Neumann conditions for the potential temperature at the bottom. An initial temperature profile is given at the beginning of the simulation with neutral conditions up to a level of 700 m followed by an inversion with a gradient of 2 K/100 m in order to allow a rapid development of convection. The second simulation of the convective boundary layer is initialized with a constant wind profile of $u = 5$ m/s. Sizes of the model domains for these two simulations are 4 km x 4 km x 1.7 km with a resolution of 2 m. A stretching of the vertical grid is done from 800 m up to the total height of the domain to save computational time. This results in a total number of 2049 x 2049 x 450 = 1.89x10^9 grid points.
The stably stratified boundary layer has a size of 800 m x 800 m x 800 m and a grid spacing of 1 m (800^3 = 0.5x10^9 grid points). The smaller domain and higher resolution is due to the smaller-scale of turbulence compared to the convective cases. The set-up of the stably stratified simulation is based on the LES intercomparison GABLS3 [13] with a realistic development of a nocturnal stably stratified boundary layer.
The large size of the model domains is required due to the fact that the largest turbulent structures of each scenario have to fit into the domain to develop a realistical flow of the atmospheric boundary layer. At the same time grid resolutions have to be fine enough to resolve turbulence which is at least one order of magnitude smaller than the wing span for later investigations of stall effects.
Simulations of atmospheric boundary layer flows including such a huge amount of grid points and high resolutions are absolutely unique. They were carried out at the HLRN (North-German Supercomputing Alliance) on the SGI Altix ICE2 system. The convective boundary layers were simulated over a period of six hours and therefore took about 4.2 days of CPU time (without mean background wind) and 5.5 days of CPU time (with mean background wind) on 2048 processors. The third simulation (stably stratified boundary layer) required three hours simulated time which results in 2.4 days of CPU time on 1024 processors. The total memory required was 2.9 TB (convective case), and 73 GB (stable case), respectively.

2.1 Virtual flight measurements

100 virtual flights are performed at ten different heights simultaneously following the method of Schröter [4]. Start heights for the virtual flights range from 50 m to 500 m within the convective boundary layer. The ratio *start height* to *boundary layer height* z_i (0.06 z_i to 0.6 z_i) is kept constant throughout the simulations in order to minimize the effects due to changes in z_i. Since the height of the stably stratified boundary layer is lower than for the convective cases, flight heights range from 50 m to 300 m. The flight heights are kept constant for the stable case because here the boundary layer height growth is much slower than for the convective boundary layers.
The virtual flights start after one hour simulated time when the turbulent flow has reached a quasi-stationary state. Values of the three wind components u, v, w and the potential temperature θ are measured after every time step with a sampling rate of ten meters (hence, the grid spacing of the virtual flights is $d_{vf} = 10$ m). This is due to the fact that turbulent elements require about five grid points to be resolved properly. With the numeric grid spacing of 2 m (respectively 1 m for the stable case) a sampling rate of ten meters (respectively five meters) is chosen for the virtually measured time series.
Since statistical properties are extracted from the virtual time series data, the statistical sig-

nificance of the virtual data are analyzed. Therefore, different averaging times are compared (up to five hours) and error margins are calculated. The longer the simulated time the better is the statistic, i.e. measurements agree better with the (horizontal) ensemble mean of the model domain and the systematic and random errors become smaller. In the convective cases covariances of the wind components require a much longer averaging time (and therefore simulated time) than variances or covariances of scalars. This is due to the fact that covariances of wind components have smaller correlation coefficients than covariances of scalars [14]. The correlation coefficients here depend on the ratio of the Monin-Obukhov length to the height of the ABL [15]. Therefore, the covariances of the mean background wind case converge slightly faster to the ensemble average than without mean background wind.
A virtual flight of two hours at a start height of 400 m (=$0.46z_i$) is chosen to generate the synthetic fields for both convective boundary layers. Statistics from these virtual time series are in good agreement with the ensemble mean.
Correlation coefficients of the wind components for the stably stratifed boundary layer are nearly one order of magnitude higher than for the convective cases. This results in much better statistics for same simulated times. A measurement time of ten minutes would be accurate enough. However, in order to have analogical approaches for all three simulated scenarios a virtual flight of one hour at a height of 125 m is used for the stably stratified boundary layer also.
The synthetic fields obtained from the chosen virtual flight measurements have a grid spacing of $d_{sf} = 17.32$ m for the convective boundary layers and $d_{sf} = 8.66$ m for the stably stratified case. This is due to the fact that the maximum wavenumber of the one-dimensional virtual measurement data ($k_{max} = 1/(2 \times d_{vf})$) has to be resolved by the three-dimensional synthetic fields ($k_{max} = \sqrt{k_{xmax}^2 + k_{ymax}^2 + k_{zmax}^2}$), this results in $d_{sf} = \sqrt{3} \times d_{vf}$. The synthetic fields have been chosen to have 500 grid points along each direction in order to get significant statistics. The domain sizes of the synthetic fields are therefore larger (8660^3 m, respectively 4330^3 m) than the simulated ones.

3 Results

Instantaneous volume data, horizontally averaged profiles and statistical properties of synthetic and explicitly simulated LES fields are analyzed and compared. The turbulent flow in the atmospheric boundary layer strongly depends on the meteorological situation and boundary conditions. The results of the comparison are therefore separately presented for the convective and the stably stratified boundary layer.

3.1 Convective boundary layer

The homogeneously heated surface of the simulated convective boundary layer causes an organized circulation pattern. In the lower boundary layer (up to 200 m) up- and downdrafts develop in hexagonal cells (a so-called spoke-like pattern). Large regions with negative vertical velocities are surrounded by narrow and strong updrafts. This typical pattern is visualized by a horizontal cross section through the entire model domain in figure 1. The vertical velocity w is shown at a height of 70 m. Red colors indicate positive and blue colors negative velocities. Strongest vertical velocities evolve in areas where spokes converge. The pattern emerges into larger-scale structures with height and the distribution of the vertical velocity changes even more to wide regions with weak downdrafts and small regions with stronger updrafts.

A vertical cross section of w (figure 2) demonstrates this distribution once again. Narrow thermals, ranging from the surface to the top of the boundary layer (around 1100 m), exhibit velocities up to 7 m/s. Corresponding downdrafts reach only -4 to -5 m/s. The top of the boundary layer is indicated by the height where up- and downdrafts become significantly weaker.

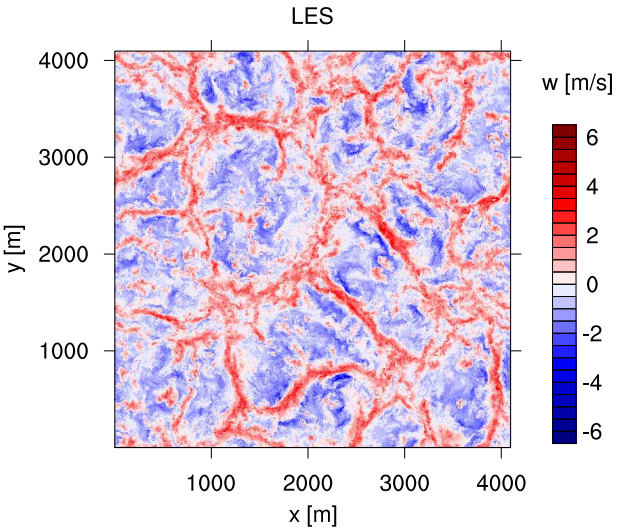

Figure 1: CBL without mean background wind; horizontal cross section of the vertical velocity w at a height of 70 m.

These typical organized structures cannot be reproduced by the synthetic field. Figure 3 shows the differences in horizontal cross sections of the explicitly simulated LES (left graphic) and the synthetic field (right graphic). The height of the explicitly simulated LES cross section is equal to the chosen virtual measurement height ($0.46 z_i$). Since turbulence in the synthetic field is isotropic, the shown cross section was chosen in the middle of the model domain. It is apparent that the coherent structures are not generated. A Gaussian distribution of the vertical velocity occurs in the synthetic field instead.

More optimistic results can be drawn from a comparison of statistical properties. The properties of the explicitly simulated LES field present the statistics in one horizontal plane (according to the height of the virtual flight measurements). Variances, covariances and correlations of the velocity components are in good agreement with the synthetic field. But

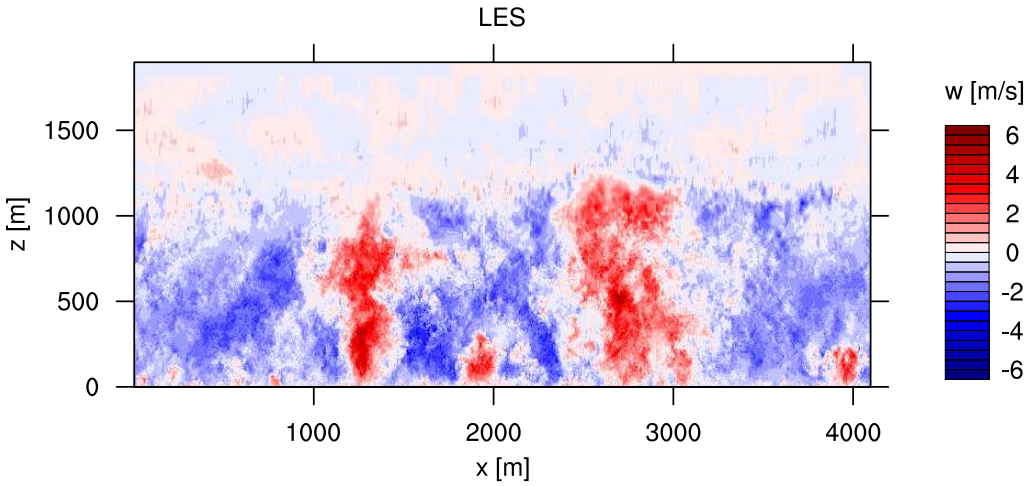

Figure 2: CBL without mean background wind; vertical cross section of the vertical velocity w at y = 640 m.

the height dependencies of these quantities cannot be reproduced since the statistics required for the generation of the synthetic fields are taken in one horizontal plane and can therefore not provide height information. Figure 4 shows profiles of the horizontally averaged vertical velocity variance w^2 plotted against the height z. The shape of the left curve reveals the typical

dependence of w^2 on height. Near the surface and the top of the boundary layer the variance w^2 is close to $0\,\mathrm{m}^2/\mathrm{s}^2$ due to small-scale turbulence. Largest structures develop slightly below the middle of the boundary layer at 0.3-0.4 z_i where a maximum of the variance w^2 occurs (here at $z = 300\,\mathrm{m}$).

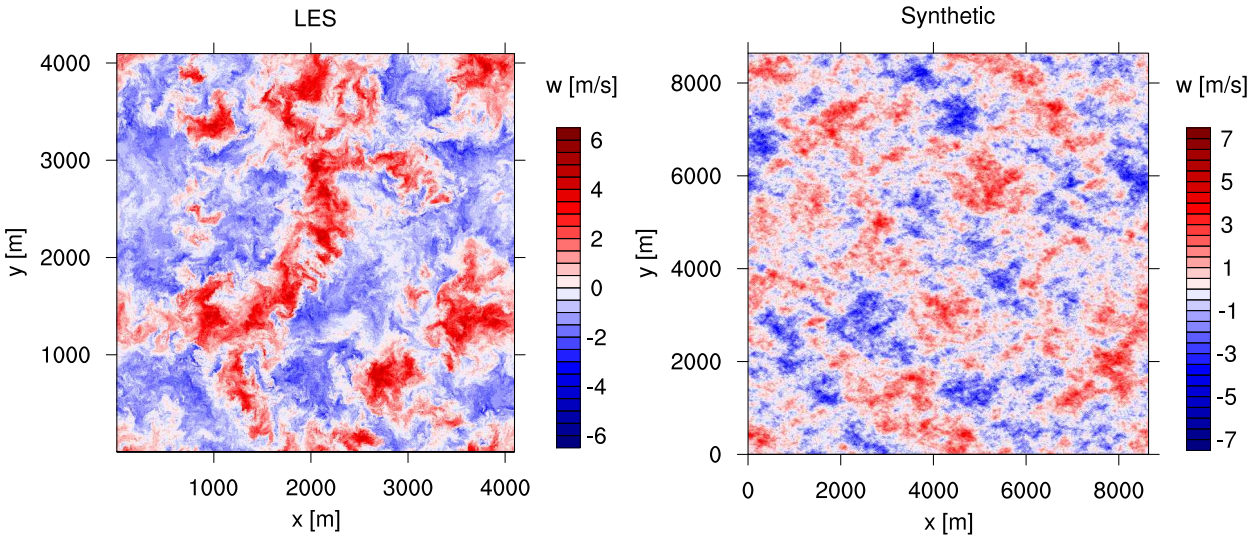

Figure 3: CBL without mean background wind; horizontal cross sections of the vertical velocity w at a height of $0.46 z_i$ for the explicitly simulated LES field and in the middle of the domain for the synthetic field.

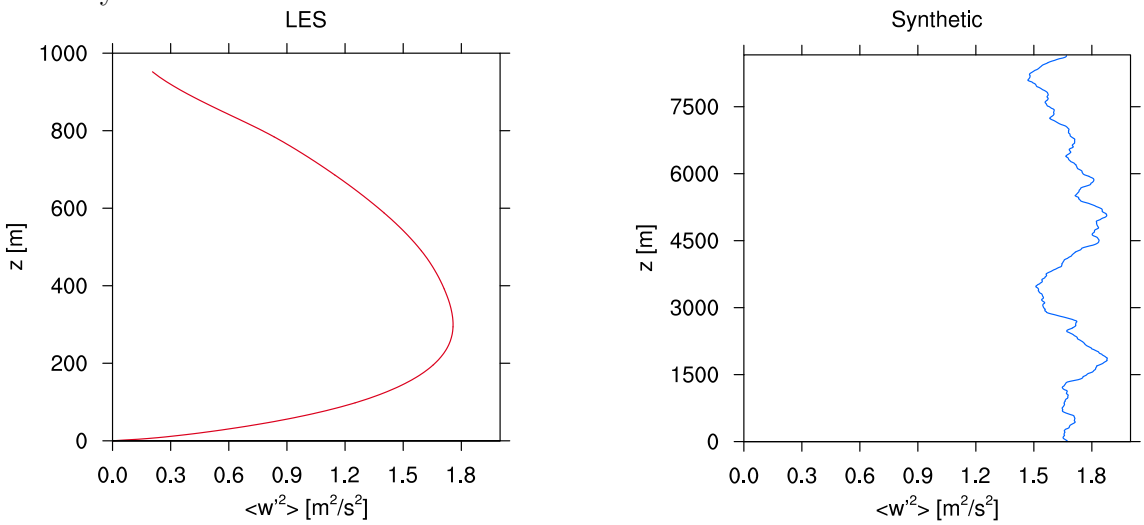

Figure 4: CBL without mean background wind; profiles of the horizontally averaged variance of w.

As expected this curve is not reproduced by the synthetic field (right graphic), w^2 only varies about the averaged value of the virtual measured time series at all heights.
Although variances, covariances or correlation coefficients calculated for one horizontal plane are in good agreement, differences can be found concerning the probability density function (PDF) of the vertical velocity. It is calculated at the height of the virtual measurement. Due to the non-Gaussian distribution of the vertical velocity component in a convective boundary layer, resulting PDFs of w have a shifted maximum (see figure 5, red curve). The maximum is moved to negative values and the curve shows a rapid sloping to zero whereas it is smoother to positive values. It reflects the typical distribution with more but weaker negative vertical velocities and

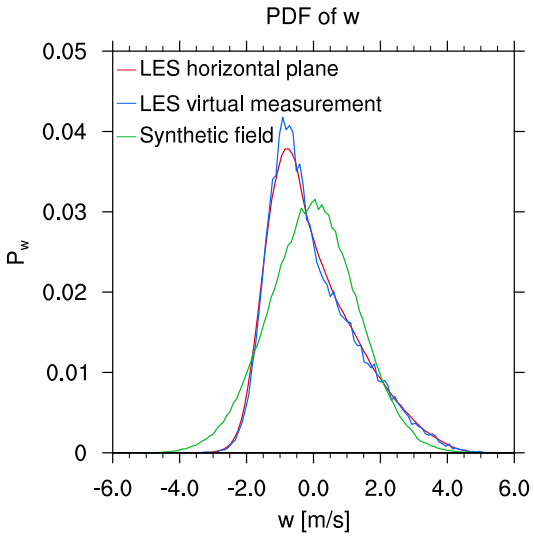

Figure 5: CBL without mean background wind; PDF of w at a height of $0.46z_i$.

less but stronger positive vertical velocities. This characteristic is also presented by the virtual time series data (blue curve). These virtual time series data are used for the generation of the synthetic field. However, the resulting synthetic fields yield a Gaussian distribution of PDFs of w (green curve) instead, which was already evident from the horizontal cross sections of w in figure 3.
The comparison of respective fields with a moderate mean background wind (not shown) yields similar results. The organized structures are just slightly modified by the mean background wind.

3.2 Stably stratified boundary layer

In contrast to the results of a convective boundary layer, the synthetic fields of a stably stratified boundary layer are in much better agreement with the explicitly simulated LES fields. Due to the stable stratification, turbulence is much weaker and vertical velocities are generally smaller than in the convective cases. More or less Gaussian-distributed turbulence develops up to the top of the stably stratified boundary layer at $z \approx 150\,\mathrm{m}$ and hence can be generated easier.
Figure 6 shows horizontal cross sections of the vertical velocity w for the explicitly simulated LES field (left graphic) and the synthetic field (right graphic). It is obvious that the structures are much smaller than in the convective cases. Both fields display a normal distribution of these small-scale turbulence.
The horizontal velocity of a stably stratified boundary layer has a special feature near the top of the boundary layer. In this region a maximum of the horizontal velocity develops, which can be twice as strong as the geostrophic wind in the free atmosphere. This maximum is the so-called low level jet. The averaged horizontal velocity $|v_{horiz}|$ reaches values up to $10\,\mathrm{m/s}$ at a height of $125\,\mathrm{m}$ as drawn in figure 7. This feature cannot be produced by the synthetic field since information on height are not provided by the virtual flight measurements taken in one horizontal plane.
In contrast to the convective boundary layers, good agreements can be achieved between PDFs of explicitly simulated LES fields, virtual measurements and synthetic fields. The distribution of w is Gaussian and can therefore be generated well. Figure 8 shows the corresponding PDFs. All three curves are in good agreement.

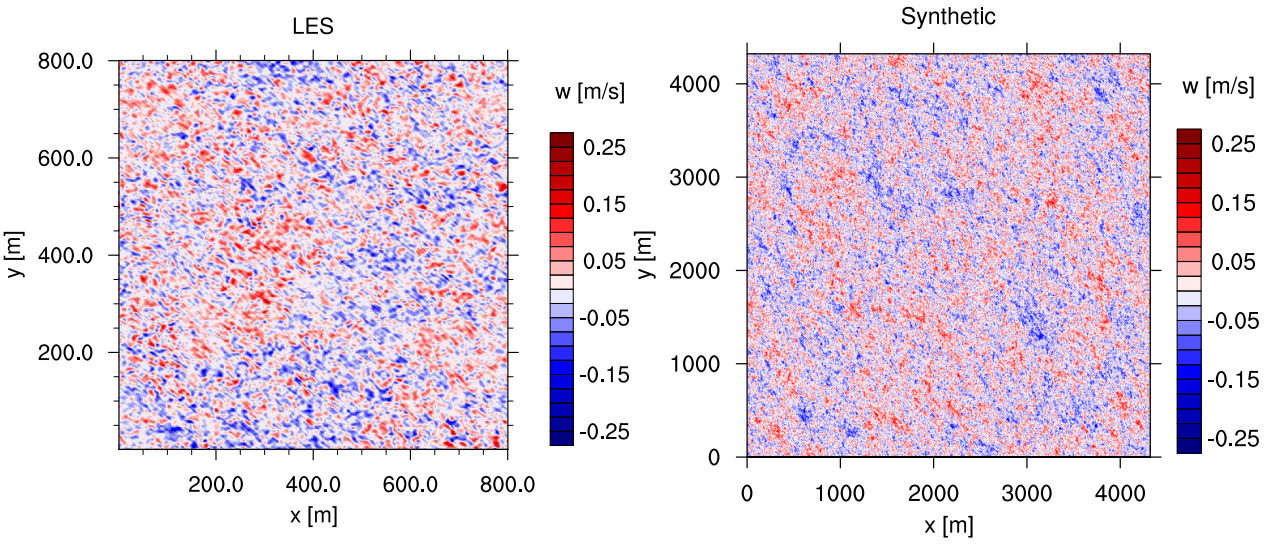

Figure 6: SBL; horizontal cross sections of the vertical velocity w at a height of $z = 125\,\mathrm{m}$ for the explicitly simulated LES field and in the middle of the domain for the synthetic field.

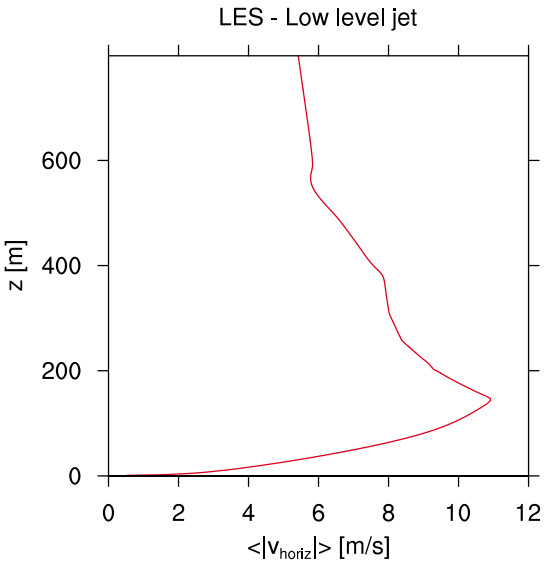

Figure 7: SBL; profile of the averaged horizontal velocity value.

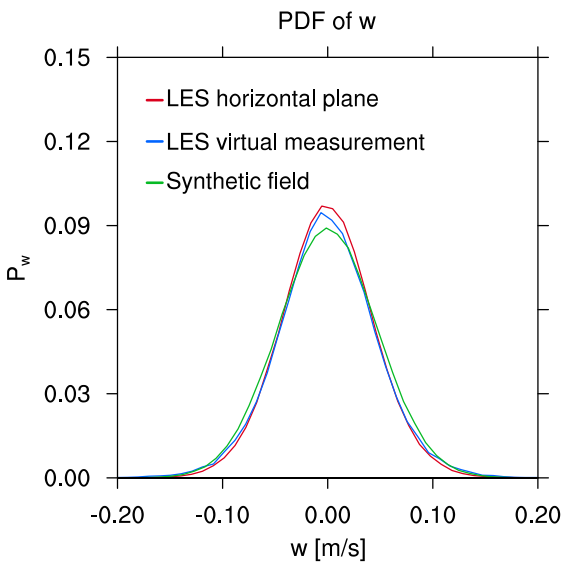

Figure 8: SBL; PDF of w at a height of $z = 125\,\mathrm{m}$.

4 Conclusion

Two different methods were developed and compared to provide three-dimensional realistic turbulent wind fields for initializing a numerical model for stall investigations. The first method uses the LES model PALM to simulate highly resolved atmospheric boundary layer flows under realistic conditions. The second one generates synthetic fields from one-dimensional flight measurements.

This study performs one-dimensional virtual flight measurements within the LES. Synthetic fields are then generated from these virtual measurement data and compared with the explicitly simulated LES fields. This approach allows us to precisely evaluate the quality of the synthetic fields, because ideally, the synthetic fields should show the same features as the explicitly simulated LES fields.

We could point out that typical three-dimensional coherent structures as developed in convective boundary layers are missing in the synthetic fields. Height dependencies of statistical properties are also not reproduced. This is nor expected since height information are not provided by the virtual flight measurements. But the synthetic fields are not able to generate the non-Gaussian distribution of the vertical velocity in one horizontal plane either. However, the second method generates realistic fields provided that the meteorological conditions lead to Gaussian-distributed turbulence as in stably stratified cases.
Both wind fields will later be used to initialize a numerical model for stall investigations in order to identify the general effects of air turbulence on wings and to find out differences caused by the two methods. Synthetic fields can be generated fast but so far we do not know if they represent atmospheric turbulence adequate enough. If huge differences will reveal, further steps have to be considered carefully. It has to be clarified, if required modifications of the synthetic method yield a better result or if only LES provides realistic three-dimensional turbulent wind fields.

Acknowledgments

The members of the FOR 1066 research group gratefully acknowledge the support of the "Deutsche Forschungsgemeinschaft DFG" (German Research Foundation) which funded this research.
We also thank the technical staff members of the North-German Supercomputing Alliance (HRLN) for assistance and support.

References

[1] Bange, J., Spieß, T., Herold, M., Beyrich, F., and Hennemuth, B., 2006. Turbulent Fluxes from Helipod Flights above Quasi-Homogeneous Patches within the LITFASS Area. Boundary-Layer Meteorol. 121, 127-151.

[2] Bange, J., Spieß, T., and van den Kroonenberg, A., 2007. Characteristics of the Early-Morning Shallow Convective Boundary Layer from Helipod Flights during STINHO-2. Theor. Appl. Climatol. 90, 113-126.

[3] Auerswald, T., Weinreis, C., Bange, J., Raasch, S., Radespiel, R., 2010. Comparison Of High Resolution Large-Eddy Simulations And Synthetic Turbulent Wind Fields. AIAA Paper 2010-1253, 48th AIAA Aerospace Sciences Meeting Including the New Horizons Forum and Aerospace Exposition. Orlando, Florida.

[4] Schröter, M., Bange, J., and Raasch, S., 2000. Simulated airborne flux measurements in a LES generated convective boundary layer. Boundary-Layer Met. 95, 437-456.

[5] Raasch, S., Schröter, M., 2001. PALM - A large-eddy simulation model performing on massively parallel computers, Meteorologische Zeitschrift 10, Number 5, 363-372.

[6] Schumann, U., 1975. Subgrid scale model for finite difference simulations of turbulent flows in plane channels and annuli. J. Comput. Phys. 18, 376-404.

[7] Deardorff, J.W., 1980. Stratocumulus-capped mixed layers derived from a three-dimensional model. Boundary-Layer Meteorol. 18, 495-527.

[8] Harlow, F.H., Welch, J.E., 1965. Numerical calculation of time-dependent viscous incompressible flow with free surface. Phys. Fluids 8, 2182-2189.

[9] Arakawa, A., Lamb, V.R., 1977. Computational design of the basic dynamical processes of the UCLA general circulation model. In: Chang, J. (Ed.), General circulation models of the atmosphere. Vol. 17 of Methods in Computational Physics. Academic Press, pp. 173-265.

[10] Piacsek, S.A., Williams, G.P., 1970. Conservation properties of convection difference schemes. J. Comput. Phys. 6, 392-405.

[11] Bott, A., 1989. A positive definite advection scheme obtained by nonlinear renormalization of the advection fluxes. Mon. Wea. Rev. 117, 1006-1015.

[12] Chlond, A., 1994. Locally modified version of Bott's advection scheme. Mon. Wea. Rev. 122, 111-125.

[13] http://www.atmo.ttu.edu/basu/GABLS3/GABLS3_LES_Revised.pdf

[14] Lenschow, D. and Stankov, B., 1986. Length scales in the convective boundary layer. J. Atmos. Sci. 43, 1198-1209.

[15] Lenschow, D., Mann, J., and Kristensen, L., 1994. How long is long enough when measuring fluxes and other turbulent statistics. J. Atmos. Oceanic Technol. 11, 661-673